Contemporary Mathematics
https://ojs.wiserpub.com/index.php/CM/

Research Article

Enhancing Voltage Stability and Power Quality in Hybrid MPPT Algorithm Based SPV-Wind Hybrid Microgrid System Tied Utility Grid Integrating Modified STATCOM

Nibedita Ghosh[1*], Asha Rani M. A.[1], Rahul Kumar[2]

[1] Department of Electrical Engineering, National Institute of Technology, Silchar, 788010, India
[2] Department of Electrical Engineering, Motilal Nehru National Institute of Technology, Allahabad, 211004, India
E-mail: gnibedita415@gmail.com

Received: 31 October 2024; **Revised:** 22 November 2024; **Accepted:** 26 November 2024

Abstract: Voltage sags can lead to equipment malfunction, decreased performance, and operational disruptions. They are typically caused by short circuits, motor start-ups, or sudden load increases, affecting power system reliability. Voltage stability of the proposed system has been improved by implementing modified Static Synchronous Compensator (m-STATCOM) by reducing voltage sags resulting power quality of the proposed system has been enhanced during breakdowns in electrical systems. The Voltage-Source Inverter (VSI) technology of m-STATCOM allows for quick reaction. At the Point of Common Coupling (PCC), it stabilizes voltage to avoid equipment damage from voltage fluctuations. m-STATCOM boosts reactive power regulation, renewable energy stability, and fault ride-through for dependable grid performance. Hybrid Incremental Conductance and Ripple Correlation Control (INC-RCC) for MPPT in PV and wind farms tracks Maximum Power Point Tracking (MPPT) under diverse situations to reduce power losses and fluctuations resulting improve efficiency and reaction speed as compared to Penguin Search (PS) optimization. System stability and performance improve with the Solar Photovoltaic (SPV)-Wind farm and Sinusoidal Pulse Width Modulation (SPWM)-Voltage Source Inverter (VSI)-based m-STATCOM controller. This integrated solution assists in minimizing LLG failure voltage drops.1KW SPV and 2.5 kW wind farm hybrid system connected to 400 V, 50 Hz utility grid integrated to the SPWM-VSI based m-STATCOM controller has been designed using MATLAB/Simulink.

Keywords: solar photovoltaic (SPV) system, static synchronous compensator (STATCOM), sinusoidal pulse width modulation (SPWM), voltage source inverter (VSI), double line to ground fault (LLG)

MSC: 93A15, 78M50, 94C05, 93C95, 93B52

Abbreviation

Symbol	Description
I_{sc}	Short circuit current (A)
G	Irradiance (W/m^2)
q	Electron charge (C)

DOI: https://doi.org/10.37256/cm.6220256003

K	Boltzmann constant
A	Ideality factor
E_g	Silicon band gap energy (J)
N_s	Number of cells connected in series
V_{OC}	Open circuit voltage (V)
T_r	Reference operating temperature (K)
R_{sh}	Parallel resistance (Ω)
R_s	Series resistance (Ω)
V_{PV}	Output voltage (V)
I_{PV}	Output current (A)
I_{ph}	Photon current (A)
I_d	Diode current (A)
I	Total current (A)
P_{wind}	Total power available from the wind (W)
m	Mass of the air (kg)
ρ	Air density (kg/m^3)
A^I	Swept area (m^2)
R	Radius of the rotor (m)
v	Wind speed (m/s)
C_p	Maximum power coefficient
λ	Tip speed ratio
ω	Rotor angular velocity (rad/s)
$\eta_{mechanical}$	Mechanical efficiency
$\eta_{electrical}$	Electrical efficiency
v_d, v_q	Voltage components in the $dq0$ frame
P	Active power (kW)
Q	Reactive power (kVAR)
m-STATCOM	Modified static synchronous compensator
VSI	Voltage-source inverter
PCC	Point of common coupling
INC-RCC	Incremental conductance and ripple correlation control
MPPT	Maximum power point tracking
PS	Penguin search
SPV	Solar photovoltaic
SPWM-VSI	Sinusoidal pulse width modulation voltage source inverter
DVC	Dual vector controller
GOA-PSO	Grasshopper optimization-particle swarm optimization
RES	Renewable energy sources
LVRT	Low voltage ride through
WECS	Wind energy conversion system
FRT	Fault ride-through
IGBT	Insulated gate bipolar transistor
MOSFET	Metal oxide semiconductor field effect transistor

1. Introduction

Voltage sag, a transient drop in voltage between 10% and 90% of nominal values, may damage electronic devices and heavy machinery. Problems, system crashes, and lost data are all possible outcomes. High power demand, electrical

failures in the power system, and short circuits are common reasons [1–3]. Power grid instability can happen when wind turbine voltage drops due to weather fluctuations. This is reduced by controlling a Series Static Synchronous Compensator with a Dual Vector Controller (DVC). By modifying reactive power, the DVC efficiently mitigates voltage dips, maintaining a steady voltage and enhancing system stability even in the face of variations [4]. Voltage sag due to faults in a utility grid connected wind farm has been investigated and mitigated by implementing hybrid Grasshopper Optimization-Particle swarm Optimization (GOA-PSO) algorithm applied on STATCOM controller [5]. Using optimization techniques for STATCOM control, a Squirrel Cage Induction Generator (SCIG) wind farm that is linked to the utility grid has been investigated.

When compared to other optimization strategies, the STATCOM controller based on the Firefly Algorithm (FA) has shown to be the most successful in regulating reactive power and voltage stability during major disturbances [6]. Alhamrouni et al. [7] introduces a STATCOM controller that optimizes the voltage profile and corrects the power factor in a utility grid linked micro grid. The controller is based on a Neural Network using simplified Space Vector Pulse Width Modulation (SVPWM). Enhancing system dependability and performance under varied situations, the controller excels at preserving grid stability during disruptions. D-STATCOM has been implemented in utility grid connected photovoltaic power plant to compensate the voltage sag, swell under fault condition and increasing inclusion of renewable energy sources (RES). Power quality of a utility grid connected micro grid has been improved [8].

Low voltage ride through (LVRT) allows power generation systems like wind turbines and solar power plants to continue operating and remain connected to the electrical grid during short periods of reduced voltage due to disturbances in the utility grid side which has been mitigated by hybrid particle swarm optimization-artificial hummingbird algorithm based STATCOM controller and it has been compared with the conventional STATCOM [9]. Micro grids are used to supply the demand of consumers who need energy from the natural sources.

Instability can occur in the utility grid connected micro grid due to frequency and voltage as there is a lack of control. In [10] battery energy storage and D-STATCOM are used to stabilize the micro grid connected utility grid. D-STATCOM can be used in conjunction with a hydrogen fuel cell to reduce voltage fluctuations caused by faults in a utility grid that is linked to the fuel cell [11]. By compensating for dynamic reactive power, D-STATCOM keeps the voltage stable even when problems occur. This synergy supports renewable integration, improves power quality, and guarantees dependable operation while strengthening the system's resilience through voltage stability maintenance in the face of fluctuating loads or grid disruptions [12]. Kilic et al. [13] discussed about the superiority of fuzzy inference system-based D-STATCOM to mitigate voltage fluctuations in the utility grid connected hydrogen fuel cell compared with the conventional PI and Adaptive Neuro Fuzzy Inference System controller. Murcia et al. [14] improve power quality by minimizing losses and enhancing voltage profiles by identifying the appropriate site for microgrids and D-STATCOMs in an IEEE 30-bus radial distribution system. A STATCOM controller also helps the system deal with power instability and voltage changes brought on by wind farms.

In addition, a PV-STATCOM uses Julia software to balance the active and reactive power in AC networks that changes dynamically. A wind energy conversion system (WECS) combined with a STATCOM linked to the utility grid has been considered for reactive power compensation and voltage stability during fault circumstances [15]. The summary is that grid-tied WECS combined with STATCOM effectively mitigates instability that happens when a fault occurs in the system between 0.8 s and 0.82 s [16]. A synchronous generator supplies both active and reactive power to an electrical grid or system. Mechanical input to the generator produces active power, which powers appliances like heaters, lights, and motors. The generator's excitation system regulates the reactive power required by inductive and capacitive components. Active and reactive power balancing is essential for grid stability and voltage control, therefore grid operators alter generator excitation systems to maintain voltage.

The fuel cell + STATCOM synchronous generator provides reactive power. The fuel cell and STATCOM controller met active and reactive power needs, respectively [17]. STATCOM controls power system voltage and reactive power. PV-STATCOM met variable reactive power requirements in this work. Capacitor bank cannot meet load-dependent reactive power. This work uses Sliding Mode Controller (SMC) + Adaptive Neuro Fuzzy Inference System (ANFIS) MPPT to maximize power during 3 ms of disturbance [18]. Power quality is how well when it meets the demands of utility-connected devices. Voltage and current waveform purity, frequency, and voltage levels are measured. Power

sources with pure sinusoidal waveform, constant voltage, and frequency are excellent. Poor power quality may damage or shorten electrical equipment. Frequency, harmonics, power factor, flicker, voltage sags, swells, and interruptions impact power quality [19]. Non-linear loads, electrical faults, large inductive or capacitive loads, and environmental factors like lightning or equipment failures can affect power quality.

In a 120 KV, 60 Hz distribution system with a 9 MW wind farm supplying a fluctuating load, Nafeh et al. [20] examined the 25 KV D-STATCOM -3MVAR to +3MVAR to stabilize voltage. This research studied utility grid-connected micro grid active and reactive power supply at steady and transient states. PV-WT-STATCOM provides additional reactive power to ensure grid voltage stability under transient state conditions on the utility grid [21]. In this proposed work it has been investigated that voltage dip occurs due to LLG fault in a 400 V, 50 Hz utility grid system connected to the load, which has been mitigated by the SPV-windfarm + PWM-VSI based m-STATCOM controller. It has been summarized that SPV-windfarm + PWM-VSI is superior to mitigate voltage dip at 400 V, 50 Hz utility grid system due to fault as compared to the system, 400 V, 50 Hz utility grid connected load without SPV-windfarm + PWM-VSI. The contributions and highlights of the Paper is described as follows:

i. Proposes a modified Static Synchronous Compensator (m-STATCOM) integrated with a Voltage-Source Inverter (VSI) to mitigate voltage sags, enhancing power quality and system reliability.

ii. Implements Hybrid INC-RCC for precise MPPT in PV and wind farms, reducing power losses and enhancing efficiency over PS optimization.

iii. Integrates m-STATCOM at PCC for rapid reactive power regulation, voltage stabilization, and fault ride-through capabilities, preventing equipment damage from voltage fluctuations.

iv. Demonstrates improved performance, stability, and response time in a 1 kW SPV and 2.5 kW wind farm hybrid system connected to a 400 V, 50 Hz utility grid, modelled in MATLAB/Simulink.

v. Shows significant voltage stability and reduced power fluctuations, supporting a reliable grid with the SPWM-VSI-based m-STATCOM controller, especially effective in minimizing LLG failure voltage drops.

The manuscript is organised as follows: Section 2 details the 1 kW SPV, 2.5 kW wind farm, and m-STATCOM, integrated with a 400 V utility grid. m-STATCOM controller using PWM-VSI technology to enhance voltage stability and power quality under dynamic conditions described in Section 3. Section 4 presents simulation in MATLAB/Simulink showing system performance improvement, reduced voltage sags, and enhanced grid stability. Finally, Section 5 summarizes the research findings, emphasizing improved voltage stability, MPPT efficiency, and grid reliability with m-STATCOM.

2. Modelling of system components

2.1 *PV mathematical modelling*

The equivalent circuit of a PV cell has been characterized in Figure 1 and the mathematical equations regarding SPV system has been represented by the following equations [22].

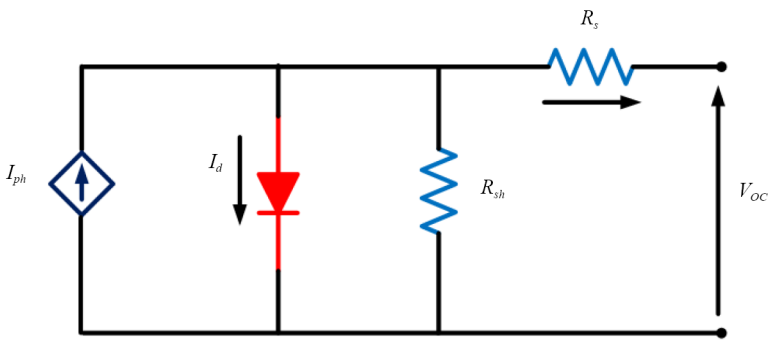

Figure 1. Equivalent circuit of SPV

$$I = I_{ph} - I_d - I_P \tag{1}$$

$$I_{ph} = \left[I_{sc} + k_i (T - T_R) \cdot \frac{G}{1{,}000} \right] \tag{2}$$

$$I_d = \left[I_s \left(\exp \left\{ \frac{q \cdot (V_{OC} + I_{PV} \times R_s)}{N_s \times A \times K \times T} \right\} \right) - 1 \right] \tag{3}$$

$$I_s = I_{rs} \cdot \left(\frac{T}{T_r} \right)^3 \cdot \exp \left(q \cdot E_g \cdot \frac{\left[\frac{1}{T_r} - \frac{1}{T} \right]}{K \times A} \right) \tag{4}$$

$$I_{rs} = \frac{I_{sc}}{\exp \left[\frac{q \cdot V_{OC}}{N_s \times A \times K \times T} \right] - 1} \tag{5}$$

$$I_p = \frac{(V_{PV} + I \cdot R_s)}{R_{sh}} \tag{6}$$

In the above equations I_{sc} represents short circuit current at standard test condition, G represents solar irradiance in W/m^2, electron charge has been represented as q is 1.6 × 10-19 C, ideality factor of silicon has been termed as A = 1.6, K = 1.3805 × 10-23 J/K represents the Boltzmann constant, T represents operating temperature, E_g = 1.12 eV which shows silicon band gap energy, N_s shows no of cells connected in series, V_{OC} represents the open circuit voltage, T_r represents reference operating temperature is 298 K.

Parallel resistance and series resistance of the equivalent circuit have been represented as R_{sh} and R_s respectively, output voltage of SPV module has been represented as V_{PV}, output current of SPV module has been termed as I_{PV}, I_{ph} represents the photon current and I_d shows the diode current, I_p term represents the current flowing through I represents the total current.

Both the PS MPPT and a hybrid INC-RCC technique form the basis of the photovoltaic (PV) measurement and load evaluation in Figure 2. The simplicity and effectiveness of PS MPPT control make it a popular choice for measuring the power peak under different circumstances and assuring steady-state performance. On the other hand, Hybrid INC-RCC MPPT control improves tracking speed and accuracy in the face of changing temperatures and irradiance by combining INC-RCC. Hybrid INC-RCC provides better flexibility to changing circumstances, according to load measurements taken under both approaches, which result in greater power stability and higher tracking accuracy.

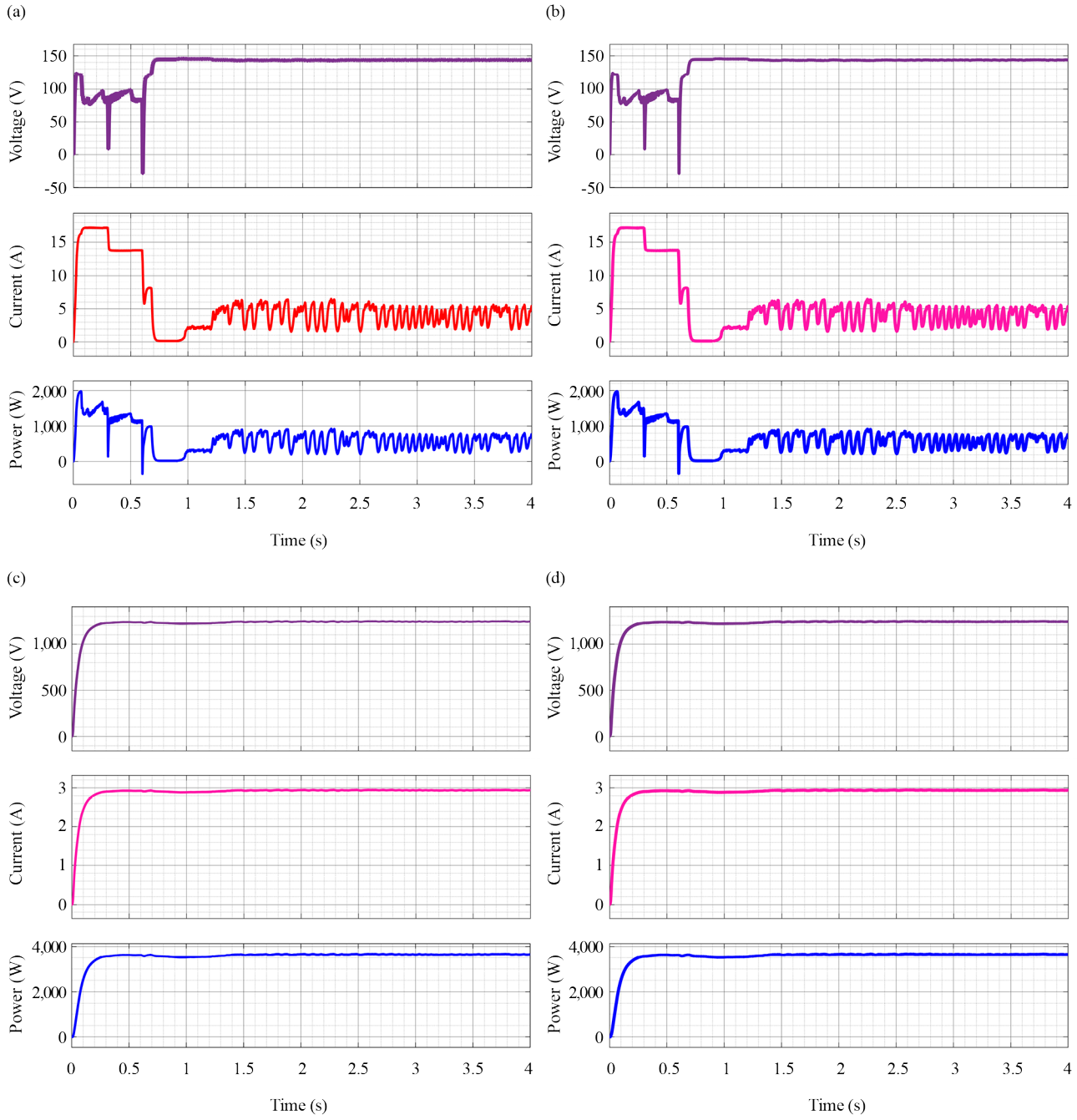

Figure 2. PV measurement based on (a) PS MPPT control, (b) Hybrid INC-RCC MPPT control. Load measurement based on (c) PS MPPT control, (d) Hybrid INC-RCC MPPT control

2.2 *Wind farm mathematical modelling*

According to the following Equation (7), the kinetic energy of the wind can be represented as [23, 24]. Kinetic energy of the wind is denoted by the symbol E_k, where m represents the mass of the air in kg and v represents the wind speed in m/s.

$$E_k = \frac{1}{2} \times m \times v^2 \tag{7}$$

The total power available from the wind, ρ is Air density (kg/m^3), typically around 1.225 kg/m^3. A^I is Swept area of the turbine R^2. Where, R is the radius of the rotor. v is the wind speed in (m/s). It is not possible to capture all the kinetic energy of wind according to Betz's law. The maximum power coefficient (C_p) is 16/27, indicating that a turbine can extract up to 16/27 of the available wind energy.

$$P_{wind} = \frac{1}{2} \times \rho \times A^I \times v^3 \tag{8}$$

The tip speed ratio λ is defined as the blade tip speed to the wind speed and it is termed as λ represents tip speed ratio, ω represents the rotor angular velocity, R is the rotor radius, v represents wind speed (m/s).

$$\lambda = \frac{\omega R}{v} \tag{9}$$

The mechanical power produced by the rotor of the turbine has been represented in Equation (10) and $n_{mechanical}$ is efficiency in mechanical. The electrical power produced from the wind farm has been represented by the Equation (11) where $n_{electrical}$ is Electrical efficiency.

$$P_{mechanical} = \frac{1}{2} \times \rho \times A \times v^3 \times c_p \times n_{mechanical} \tag{10}$$

$$P_{electrical} = \frac{1}{2} \times \rho \times A \times v^3 \times c_p \times n_{mechanical} \times n_{electrical} \tag{11}$$

Two distinct Maximum Power Point Tracking (MPPT) control approaches, PS-MPPT and INC-RCC MPPT, are shown in Figure 3 contrasting the performance of generator voltage and current and wind voltage, current, and power. The generator and wind parameters show steady-state behaviour under PS MPPT control, although can converge to the maximum power point more slowly. Whereas the Hybrid INC-RCC MPPT control approach allows for quicker and more accurate tracking, it optimizes the extraction of electricity from wind energy and improves the efficiency of generators. To achieve the best possible voltage, current, and power outputs, this hybrid method improves responsiveness even when the wind speed and direction are unpredictable.

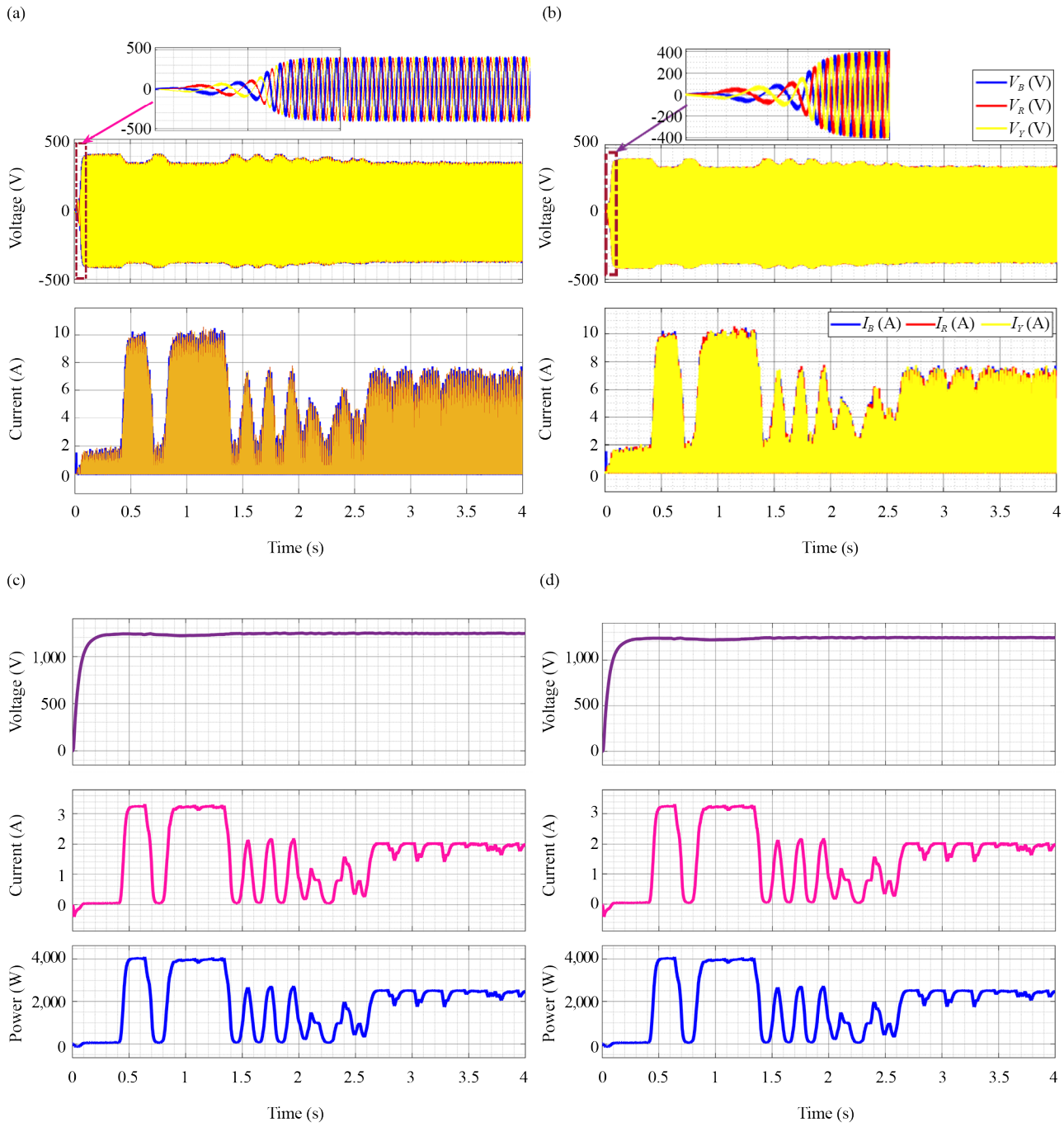

Figure 3. Generator voltage and current based on (a) PS MPPT control, (b) Hybrid INC-RCC MPPT control. Wind voltage, current, and power based on (c) PS MPPT control, (d) Hybrid INC-RCC MPPT control

2.3 *Voltage dip occurs due to fault in the system*

Voltage sag is a sudden and dramatic change of voltage due to current flow caused by the faults in the power system [25–27]. Figure 4 shows that low impedance paths are the consequence of electrical currents being redirected due to a short circuit, phase-to-phase faults, or three-phase faults [28–30]. Transmission lines, cables, and transformers are susceptible

to overheating, insulation failure, power quality concerns, and other problems as a result of the voltage drop caused by the surge in current, which occurs either throughout the system or at the fault location.

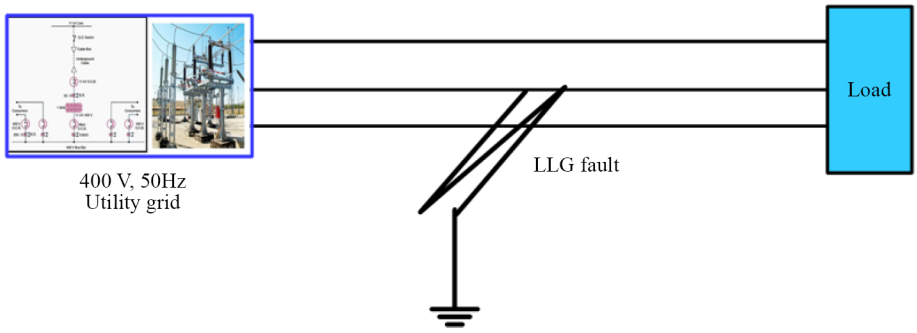

Figure 4. LLG occurs in the system

Higher current causes larger voltage drops which reduces voltage at the other part of the network [31]. During fault, generators in large power system may experience a temporary imbalance between generated and demanded power, causing a voltage drop [32]. STATCOM is a controller which regulates voltage in power systems, mitigating voltage sags caused by system faults through fast and dynamic reactive power control [33]. Voltage sag during a fault is often caused by an increase in current flow, reducing system voltage. A STATCOM controller can inject reactive power to restore voltage, boosting voltage at the point of common coupling. Its fast response time helps counteract voltage dips and stabilize the system. The STATCOM controller, installed at the PCC, stabilizes voltage at the grid interface by injecting reactive power in case of a fault, and maintains acceptable voltage levels through Automatic Voltage Regulation (AVR). STATCOM controllers use Voltage Source Converter (VSC) technology to manage voltage sags caused by faults.

Common control strategies include Proportional-Integral (PI) control, Feed forward Control, and Decoupled Control of Active and Reactive Power. PI control maintains system voltage by regulating reactive power injection, Feed forward Control predicts power demand, and the STATCOM controller can quickly inject reactive power without affecting the active power balance in the system by decoupling the control of active and reactive power. STATCOM controller mitigates voltage sag and filters harmonics from faults or switching devices, improving power quality by removing distortions in the voltage waveform. STATCOM enhances fault ride-through (FRT) for renewable energy sources like wind farms and solar PV systems connected to the utility, compensating for voltage dips during faults, preventing cascading failures in the power system.

3. Proposed m-STATCOM based PWM-VSI controller

PWM-VSI, is an essential component of power electronics for regulated voltage and frequency conversion from DC to AC. Power electronic switches, such as IGBTs or MOSFETs, are used to accomplish this transformation. Three of the most PWM approaches include sinusoidal, space vector, and hysteresis. Some of the parts used in the process include filters, loads, PWM control, switching devices, and DC input. The advantages include better control, more efficiency, and higher quality output. By simplifying the integration of renewable energy sources, energy storage systems, and loads in microgrid applications, the PWM-VSI improves the grid's overall performance and dependability. The VSI ensures proper synchronization, voltage regulation, and power flow control between the micro grid and utility grid by implementing Phase Locked Loop in the proposed system. In this proposed system, to obtain high quality AC power from the SPV wind hybrid micro grid, modified PWM-VSI has been implemented.

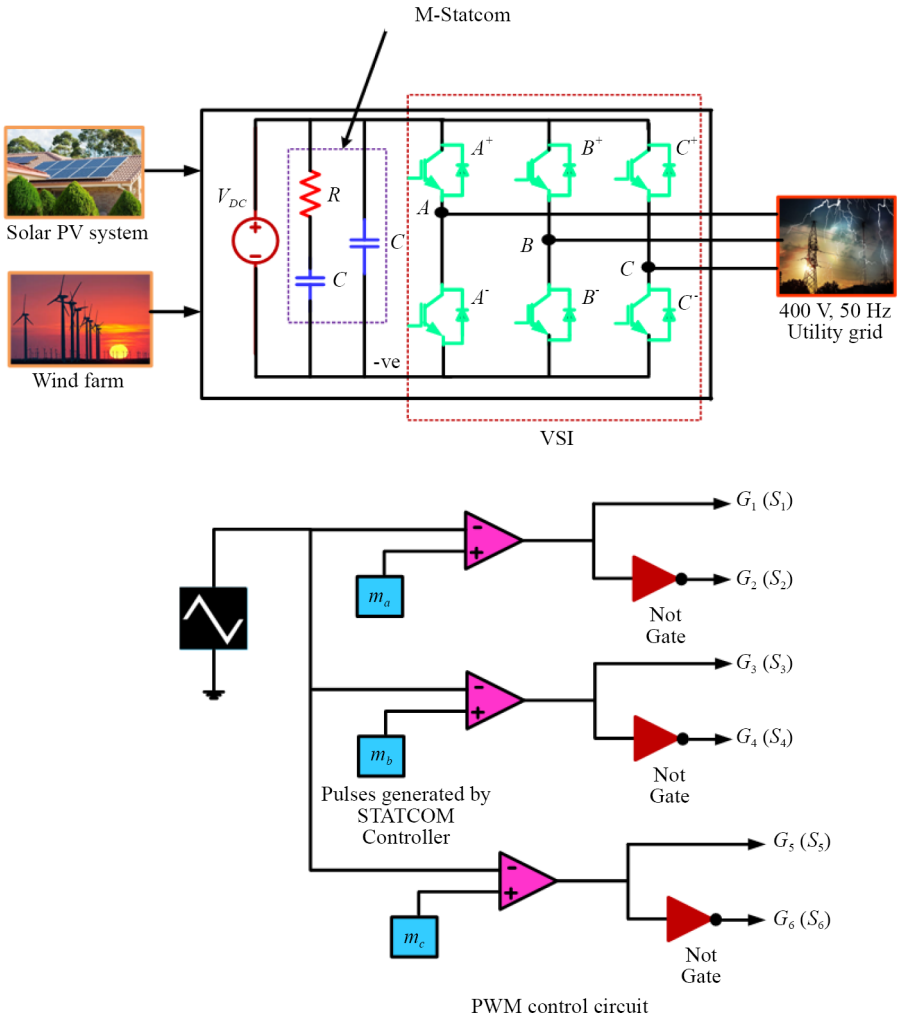

Figure 5. SPWM-VSI connected utility grid

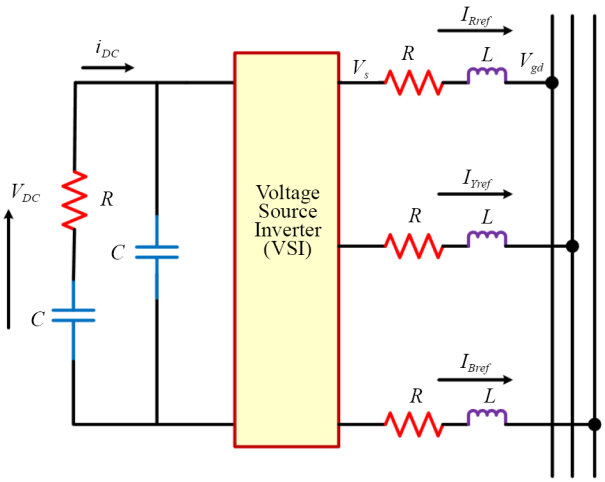

Figure 6. Proposed m-STATCOM based VSI

It results a pure sinusoidal wave after implementing *L-R* filter which has been connected between the output of PWM-VSI and 400 V, utility grid. In the proposed hybrid micro grid system, a 1 kW solar photovoltaic (SPV) input and a 2.5 kW wind farm are utilized. The system uses a modified PWM-VSI in which a reference signal generated by a fractional-order based STATCOM controller from Figures 5 and 6 is compared to a high-frequency 5 kHz triangular carrier wave.

This configuration generates gating pulses for the IGBTs arranged in a bridge setup, delivering a stable output via an LR filter connected at the midpoints of the IGBT switches. The system features a DC input voltage of 926.2 V and a 4,000 μF capacitor to minimize voltage fluctuations due to the variable nature of solar and wind energy sources.

3.1 *Controlling active and reactive power using decoupled control*

In this proposed system, inverter's output current has been divided into two components: d-axis current (controlling active power) and q-axis current (controlling reactive power). By controlling these components separately, the VSI can regulate both active and reactive power, crucial for grid stability. The active power (P) and reactive power (Q) have been represented by the $dq0$ frame.

$$P = \frac{3}{2} v_d i_d \tag{12}$$

$$Q = \frac{3}{2} v_q i_q \tag{13}$$

In Equations (12) and (13) v_d and v_q represent the voltage components in the $dq0$ frame. In this proposed system, the flow of active power can be controlled through the modified PWM-VSI inverter by regulating direct axis current (i_d) between the SPV wind hybrid micro grid and 400 V utility grid. It allows more active power to be supplied into the utility grid by increasing id and to manage reactive power by controlling i_q. The traditional abc frame's AC signals, which are challenging to control with feedback loops, can be simplified by applying the $dq0$ transformation. The Proportional Integral (PI) controllers in VSI control perform better in $dq0$ frame by regulating dc quantities, ensuring faster and more accurate dynamic power regulation. Grid connected inverters require precise control of active and reactive for maintaining power quality. The $dq0$ transformation enables quick response to power demand, voltage fluctuations, and renewable generation variation. The VSI must synchronize with the utility grid voltage and frequency using $dq0$ transformation, simplifying phase angle detection. Aligning the d-axis with the grid voltage vector maximizes active power (P), maintaining orthogonal q-axis for reactive power (Q) control.

The PWM-VSI generates switching signals by comparing a reference waveform with a 5 KHz triangular carrier waveform. Implementing $dq0$ control, the reference waveform has been derived from $dq0$ based m-STATCOM controllers. An inverse $dq0$ transformation converts DC control signals into AC signals for PWM modulation. The Park transformation transforms three-phase time-varying quantities from an abc frame into $dq0$ components in a rotating reference frame, simplifying control strategies like Proportional-Integral (PI) control.

$$\begin{bmatrix} d \\ q \\ 0 \end{bmatrix} = T(\theta) \quad \begin{bmatrix} a \\ b \\ c \end{bmatrix} \tag{14}$$

d-axis is representing the direct axis component (aligned with the reference voltage or current vector), q-axis is representing the quadrature component (90° phase shift from the d-axis), 0-axis is representing the zero-sequence component (used to handle unbalanced systems). θ represents the angular position of the rotating reference frame, often determined by the system's synchronous frequency. a, b, c are representing the three-phase (abc) signals (voltages or cur-rents). d, q, 0 reference frames are representing the components in direct axis, quadrature axis and zero sequence

components. θ represents the angular position of the rotating reference frame which has been determined by the frequency of the system. Park Transformation has been represented by $[T(\theta)]$. Inverse Park transformation is applied to convert the $dq0$ components back into the three-phase abc system.

$$\begin{bmatrix} a \\ b \\ c \end{bmatrix} = \begin{bmatrix} \cos\theta & -\sin\theta & 1 \\ \cos\left(\theta - \frac{2\pi}{3}\right) & -\sin\left(\theta - \frac{2\pi}{3}\right) & 1 \\ \cos\left(\theta + \frac{2\pi}{3}\right) & -\sin\left(\theta + \frac{2\pi}{3}\right) & 1 \end{bmatrix} \begin{bmatrix} d \\ q \\ 0 \end{bmatrix} \tag{15}$$

3.2 *Proposed m-STATCOM based modified PWM-VSI mechanism to mitigate voltage swell and voltage swag*

Table 1 depicts the algorithm for the proposed hybrid Incremental Conductance and Ripple Correlation Control-based MPPT algorithm for the SPV and wind farm, integrated with a Pulse Width Modulation (PWM)-VSI-based modified-STATCOM controller to mitigate voltage swell and voltage sag.

4. Simulation results and discussion

Active and reactive power regulation reduces voltage sag during power system breakdowns, stabilizes the system, and protects sensitive equipment. Reactive power (Q) adjusts voltage, whereas active power (P) powers lights, heating, and motors. Faults may aggravate power imbalance-induced voltage drops. Mismatched generation and demand may disrupt grids. A Line-Line-Ground (LLG) fault occurs in the 400 V, 50 Hz electrical grid that is linked to the load in the proposed system. This fault lasts for around 0.3 to 0.45 s. The voltage profile of the system drops significantly during this time because of the malfunction. During these types of issues, voltage drops generally occur because current demand is higher than usual. In order to stabilize the voltage and prevent these dips, reactive power (Q) is crucial. The proposed m-STATCOM facilitates voltage profile restoration and fault mitigation by injecting reactive power into the grid. In order to stabilize active power and reduce frequency instability, the system makes use of sophisticated control techniques and energy storage. In order to keep the grid stable and reduce voltage dips caused by faults, reactive power regulation with advanced control technology has been implemented.

The system must be able to quickly compensate for disruptions, as seen by the voltage drop in Figure 7. After implementing modified PWM-VSI based m-STATCOM controller and SPV wind based micro grid, it dynamically injects reactive power during faults to stabilize voltage and reduce sag for that duration and represented in Figure 8. LLG fault requires significant reactive power to compensate for lost voltage, enabling faster recovery and maintaining voltage stability for connected loads. The proposed m-STATCOM in a hybrid micro grid with SPV and wind energy reduces voltage sag during LLG failures. The system maintains ideal voltage levels even during disruptions using dynamic reactive power assistance. The rapid reaction time of m-STATCOM helps offset voltage swings, boosting system dependability. It also eliminates harmonics and renewable source integration. During faults, m-STATCOM improves hybrid micro grid resilience by effectively regulating reactive power flow as depicted in Figure 8.

Table 1. Proposed m-STATCOM based modified PWM-VSI pseudo code

Initialize system parameters:
Set voltage reference (V_{ref}), current reference (I_{ref}), switching frequency, and sampling time
Define control gains for voltage and current controllers
Set initial conditions for system variables (voltage, current, phase angle)
Start main control loop:
While (system is active):
Measure AC system parameters:
Measure line voltage (V_{line}) and line current (I_{line})
Calculate instantaneous reactive power (Q) using measured values
Calculate error signals:
Voltage error = V_{ref}-Initialize system parameters:
Set voltage reference (V_{ref}), current reference (I_{ref}), switching frequency, and sampling time
Define control gains for voltage and current controllers
Set initial conditions for system variables (voltage, current, phase angle)
Start main control loop:
While (system is active):
Measure AC system parameters:
Measure line voltage (V_{line}) and line current (I_{line})
Calculate instantaneous reactive power (Q) using measured values
Calculate error signals:
Voltage error = $V_{ref} - V_{line}$
Current error = $I_{ref} - I_{line}$
Apply modified PWM control using m-STATCOM:
Compute phase angle for voltage reference based on voltage and current error
Calculate duty cycle using modified PWM control law to adjust VSI output
Adjust VSI switching based on duty cycle to match desired reactive power and balance current
Update control actions:
Update m-STATCOM output voltage based on modified PWM duty cycle
Control phase angle to ensure reactive power compensation meets the desired reference
Update system states for next iteration
End While
Stop system and log performance data
Current error = $I_{ref} - I_{line}$
Apply modified PWM control using m-STATCOM:
Compute phase angle for voltage reference based on voltage and current error
Calculate duty cycle using modified PWM control law to adjust VSI output
Adjust VSI switching based on duty cycle to match desired reactive power and balance current
Update control actions:
Update m-STATCOM output voltage based on modified PWM duty cycle
Control phase angle to ensure reactive power compensation meets the desired reference
Update system states for next iteration
End While
Stop system and log performance data

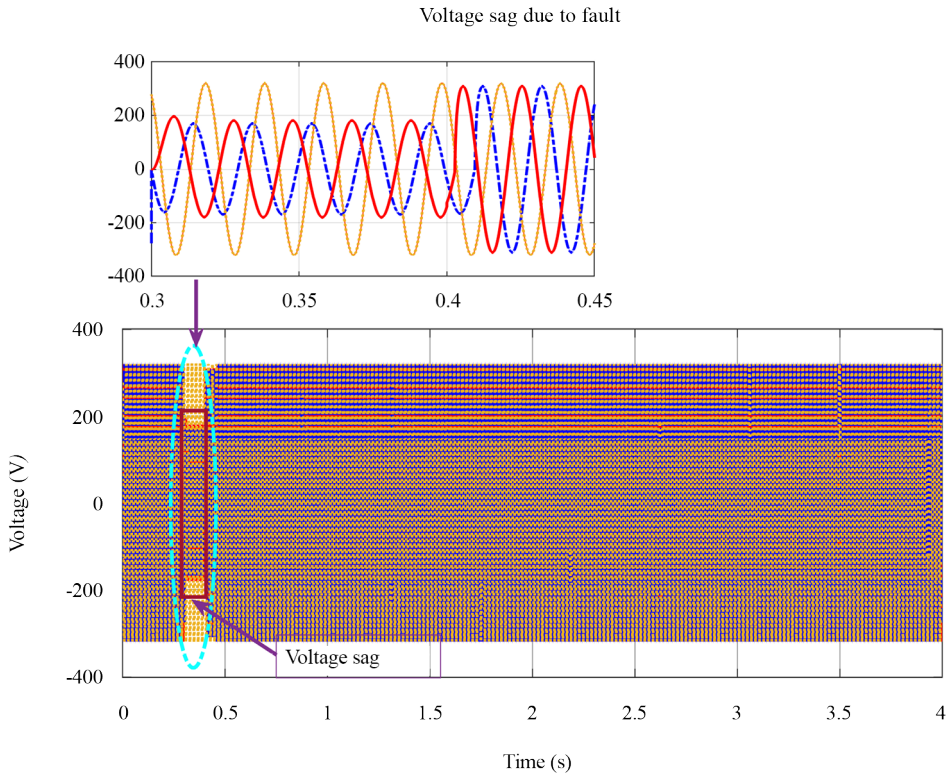

Figure 7. Voltage sag occurs in a utility grid system due to LLG fault without implementation STATCOM + SPV Wind hybrid micro grid

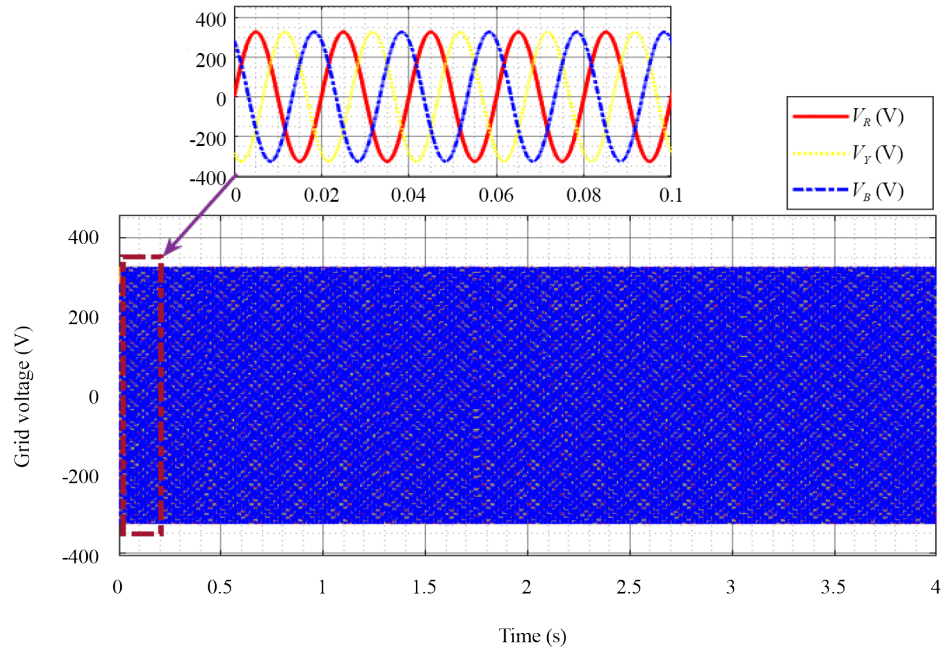

Figure 8. Voltage sag mitigation occurs in a utility grid system during LLG fault after implementation of m-STATCOM + SPV Wind hybrid microgrid

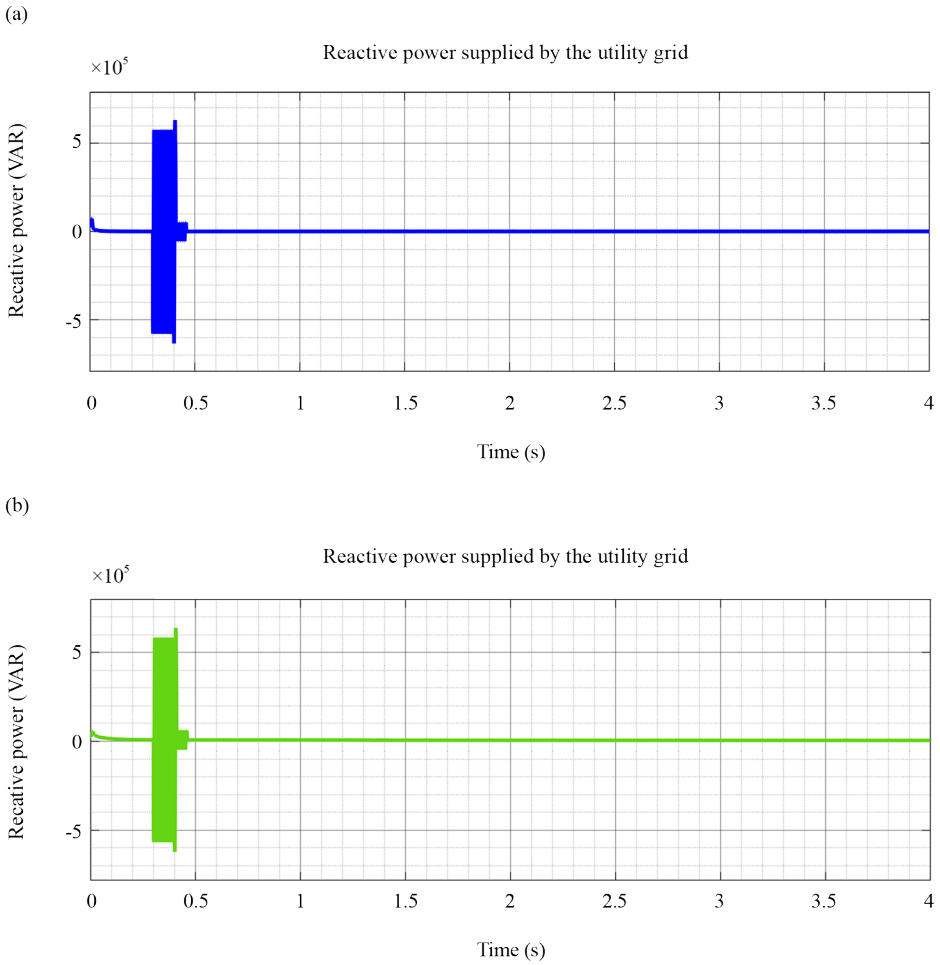

Figure 9. Reactive power supplied by the utility grid to the load for SPV + Wind farm based MPPT control for (a) PS, and (b) Hybrid INC + RCC with m-STACOM and modified PWM-VSI

Using diverse control algorithms, SPV and wind farm-based MPPT control can successfully manage utility grid reactive power to the load. Reactive power changes can be less sensitive to dynamic load situations in Penguin Search than in Hybrid INC + RCC. By immediately adjusting to changing grid circumstances, the Hybrid INC + RCC with m-STATCOM and modified PWM-VSI manages reactive power efficiently in Figure 9. During voltage sag, the m-STATCOM actively injects or absorbs reactive power to stabilize voltage. This boosts system dependability and power quality. Integrated modified PWM-VSI reduces harmonic distortion, resulting in cleaner power output. As a result, m-STATCOM makes renewable energy systems more robust to disruptions and increases grid stability. The active power supplied by the utility grid to the load for a combined SPV and wind farm setup can be influenced significantly by MPPT control strategies employed. For the PS method, power delivery can experience fluctuations due to its slower convergence to MPPT as shown in Figure 9(a), resulting in potential inefficiencies.

In contrast, according to Figure 9(b) the hybrid INC and RCC approach, when integrated with a m-STATCOM and modified PWM-VSI, offers enhanced stability and efficiency. The proposed m-STATCOM provides rapid reactive power compensation, helping to mitigate voltage sags, thus ensuring a consistent active power supply to the load as shown in Figure 10(a, b). Its ability to dynamically respond to grid disturbances and enhance power quality leads to reduced losses and improved reliability in energy delivery, making it an invaluable asset in renewable energy integration systems. The hybrid control method operates because the load absorbs active power for SPV and wind farm-based MPPT control utilizing m-STATCOM and modified PWM-VSI. By dynamically controlling reactive power to load fluctuations,

the m-STATCOM improves voltage stability and power quality. m-STATCOM also integrates renewable energy sources smoothly, preventing power supply disruptions from solar irradiance and wind speed changes. Energy efficiency has been improved by the hybrid INC and RCC algorithms, which maximize power point tracking. Using modified PWM for inverter control, m-STATCOM reduces harmonic distortion and cleans power output as shown in Figure 11(a, b). These capabilities make m-STATCOM vital for contemporary micro grids, improving dependability and efficiency.

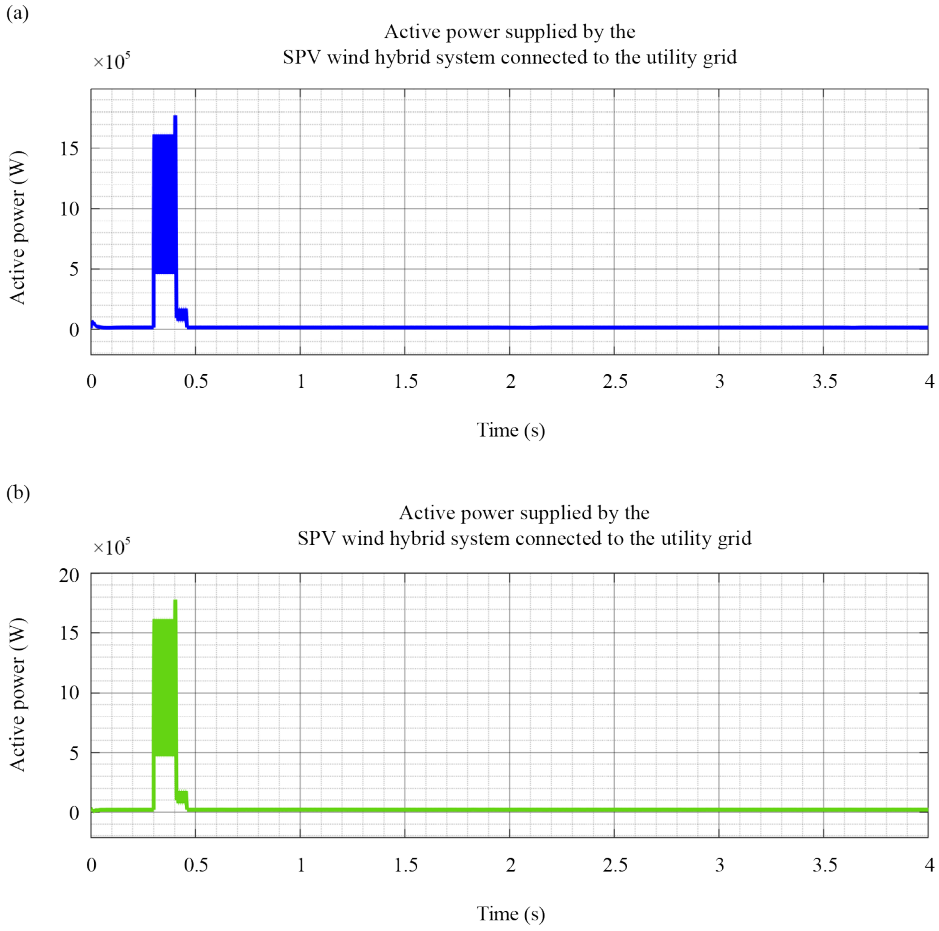

Figure 10. Active power supplied by the utility grid to the load for SPV + Wind farm based MPPT control for (a) PS, and (b) Hybrid INC + RCC with m-STACOM and SPWM-VSI

Reactive power absorbed by the load for SPV and wind farm-based MPPT control can significantly impact system performance. For PS MPPT, the reactive power management is less adaptive, potentially leading to voltage instability as depicted in Figure 12(a). In contrast, using a hybrid INC and RCC approach with proposed m-STATCOM and modified PWM-VSI offers better voltage regulation and reactive power compensation as depicted in Figure 12(b). Recompenses of proposed m-STATCOM include rapid response to voltage fluctuations, enhanced voltage stability, and the ability to mitigate voltage sags. This ensures efficient energy utilization, reduces losses, and enhances the overall reliability of the power system. Table 2 shows the simulation results of the existing work summary.

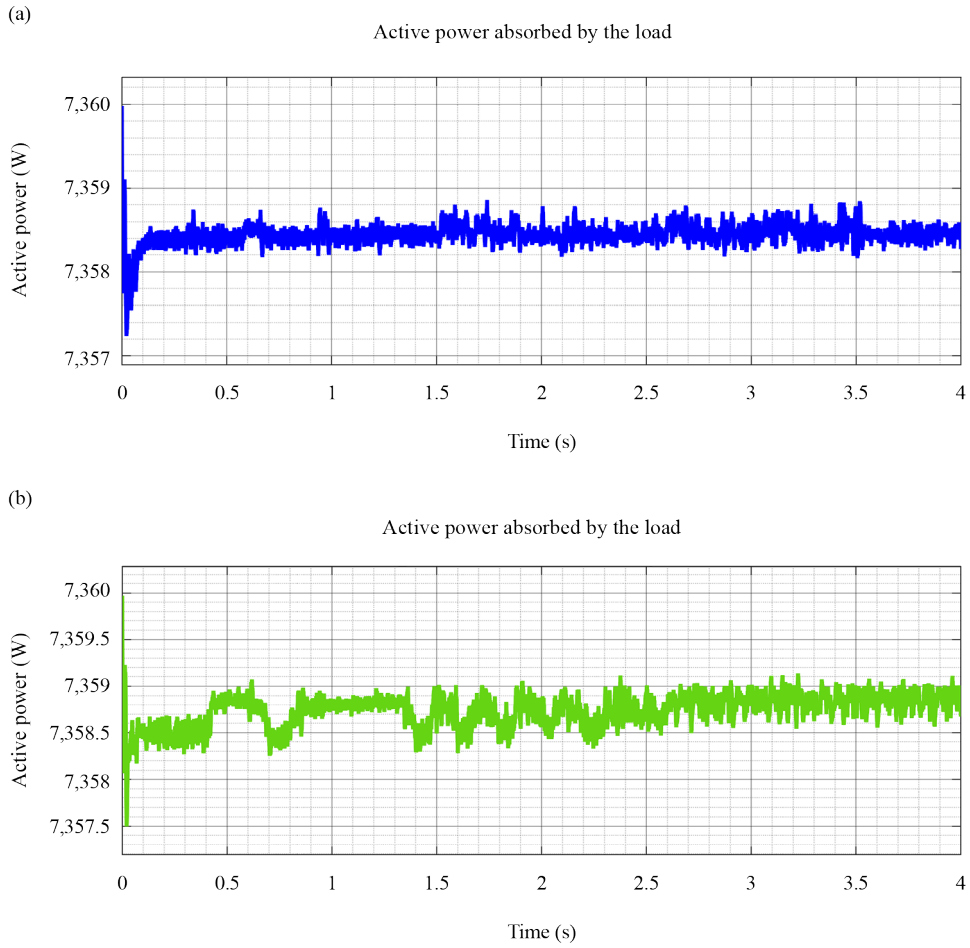

Figure 11. Active power absorbed by the load for SPV + Wind farm based MPPT control for (a) PS, and (b) Hybrid INC + RCC with m-STACOM and SPWM-VSI

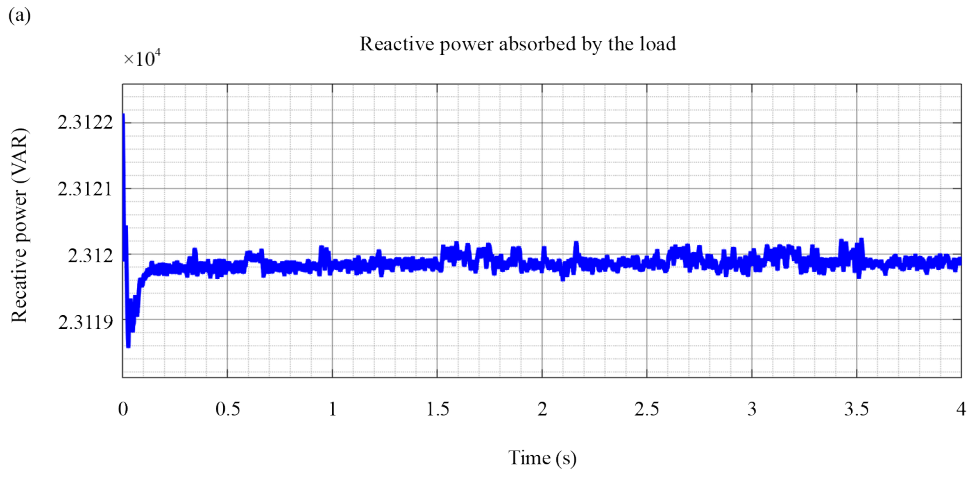

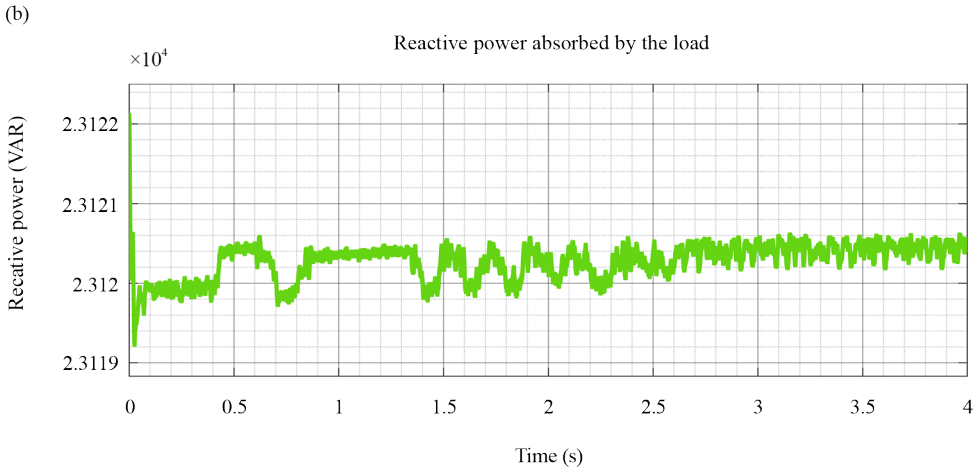

Figure 12. Reactive power absorbed by the load for SPV + Wind farm based MPPT control for (a) PS, and (b) Hybrid INC + RCC with m-STACOM and SPWM-VSI

Table 2. Summarizing the simulation results based on proposed and existing work

Algorithm	P_s (W)	Q_s (VAR)	P_{abs} (W)	Q_{abs} (VAR)
Hybrid INC-RCC based m STATCOM-modified PWM-VSI	15.12×10^5	0.0001×10^5	7,359	2.304
PS based STATCOM-PWM-VSI	15×10^5	0.0098×10^5	7,358	2.312
RCC based STATCOM-PWM-VSI	14.65×10^5	0.0085×10^5	7,265	2.126

5. Conclusions and future scope

Improved power quality, less voltage drops, and more stable voltages during power outages are all benefits of m-STATCOM, which is explained in this paper. To safeguard equipment from voltage fluctuations, its VSI technology allows for quick reaction at the PCC. When it comes to dependable grid performance, m-STATCOM improves reactive power regulation, renewable energy stability, and fault ride-through capabilities. In PV and wind farm systems, the Hybrid INC-RCC method for MPPT significantly improves efficiency and decreases power losses as compared to PS optimization. In order to reduce voltage dips caused by LLG failure, a MATLAB/Simulink simulation was run on a hybrid system that included a 1 kW SPV and a 2.5 kW wind farm. The system was linked to a 400 V, 50 Hz utility grid and used a modified PWM-VSI based m-STATCOM controller. The table compares the performance of two control strategies for a STATCOM integrated with a PWM-VSI.

The Hybrid INC-RCC based STATCOM-modified PWM-VSI shows a slightly higher active power output of 7,359 W compared to the PS-based STATCOM-PWM-VSI, which delivers 7,358 W. However, Q_s for the Hybrid INC-RCC method is significantly lower (0.0001×10^5 VAR) compared to the PS-based method (0.0098×10^5 VAR). This indicates better efficiency and reduced reactive power in the Hybrid INC-RCC strategy. P_{abs} and Q_{abs} values are almost identical for both methods, with the Hybrid INC-RCC method demonstrating a slight improvement in overall performance. These results suggest that the Hybrid INC-RCC based approach provides marginally better performance in terms of active and reactive power handling, making it more suitable for grid integration and efficiency optimization in dynamic load conditions.

Research in the future can focus on improving the m-STATCOM fault detection techniques, real-time response optimization for different grid situations, and adaptive control strategies for various renewable energy sources. Further research on the effects of scalable hybrid systems on microgrid stability can improve smart grids energy efficiency and dependability.

Conflict of interest

The authors declare no competing financial interest.

References

[1] Liubčuk V, Radziukynas V, Kairaitis G, Naujokaitis D. Power quality monitors displacement based on voltage sags propagation mechanism and grid reliability indexes. *Applied Sciences*. 2023; 13(21): 11778. Available from: http://dx.doi.org/10.3390/app132111778.

[2] Kucuk S, Ajder A. Analytical voltage drop calculations during direct on line motor starting: Solutions for industrial plants. *Ain Shams Engineering Journal*. 2022; 13(4): 101671. Available from: http://dx.doi.org/10.1016/j.asej.2021.101671.

[3] Abdelaal AK, Shaheen AM, El-Fergany AA, Alqahtani MH. Sliding mode control based dynamic voltage restorer for voltage sag compensation. *Results in Engineering*. 2024; 24: 102936. Available from: http://dx.doi.org/10.1016/j.rineng.2024.102936.

[4] Lee HP, DSouza K, Chen K, Lu N, Baran M. Adopting dynamic VAR Compensators to mitigate PV impacts on unbalanced distribution systems. *arXiv*. 2023. Available from: http://arxiv.org/abs/2309.06098.

[5] Yameen MZ, Lu Z, Rao MAA, Mohammad A, Nasimullah, Younis W. Improvement of LVRT capability of grid-connected wind-based microgrid using a hybrid GOA-PSO-tuned STATCOM for adherence to grid standards. *IET Renewable Power Generation*. 2024; 18(15): 3218-3238. Available from: https://doi.org/10.1049/rpg2.13036.

[6] Subramanian K, Loganathan AK. Voltage stability analysis of smart distribution grids with PV systems using fuzzy logic controller with firefly optimisation algorithm. *International Journal of Engineering Systems Modelling and Simulation*. 2023; 14(3): 125-140. Available from: http://dx.doi.org/10.1504/ijesms.2023.13179.

[7] Alhamrouni I, Abdul Kahar NH, Salem M, Swadi M, Zahroui Y, Kadhim DJ, et al. A comprehensive review on the role of artificial intelligence in power system stability, control, and protection: Insights and future directions. *Applied Sciences*. 2024; 14(14): 6214. Available from: http://dx.doi.org/10.3390/app14146214.

[8] Rastogi M, Ahmad A, Bhat AH. Performance investigation of two-level reduced-switch D-STATCOM in grid-tied solar-PV array with stepped P&O MPPT algorithm and modified SRF strategy. *Journal of King Saud University-Engineering Sciences*. 2021; 35(6): 393-405. Available from: http://dx.doi.org/10.1016/j.jksues.2021.06.008.

[9] Imtiaz S, Yang L, Azib Khan HM, Mudassir Munir H, Alharbi M, Jamil M. Wind-assisted microgrid grid code compliance employing a hybrid Particle swarm optimization-Artificial hummingbird algorithm optimizer-tuned STATCOM. *Wind Energy*. 2024; 27(7): 711-732. Available from: http://dx.doi.org/10.1002/we.2908.

[10] Ahmed T, Waqar A, Al-Ammar EA, Ko W, Kim Y, Aamir M. Energy management of a battery storage and D-STATCOM integrated power system using fractional order sliding mode control. *CSEE Journal of Power and Energy Systems*. 2021; 7(5): 996-1010. Available from: http://dx.doi.org/10.17775/cseejpes.2020.02530.

[11] Bayrak G, Yılmaz A, Demirci E. Fault ride-through capability enhancement of hydrogen energy-based distributed generators by using STATCOM with an intelligent control strategy. *International Journal of Hydrogen Energy*. 2023; 48(99): 39442-39462. Available from: http://dx.doi.org/10.1016/j.ijhydene.2023.06.274.

[12] Hernández-Mayoral E, Madrigal-Martínez M, Mina-Antonio JD, Iracheta-Cortez R, Enríquez-Santiago JA, Rodríguez-Rivera O, et al. A comprehensive review on power-quality issues, optimization techniques, and control strategies of microgrid based on Renewable Energy Sources. *Sustainability*. 2023; 15(12): 9847. Available from: http://dx.doi.org/10.3390/su15129847.

[13] Kilic H, Asker ME, Haydaroglu C. Enhancing power system reliability: Hydrogen fuel cell-integrated D-STATCOM for voltage sag mitigation. *International Journal of Hydrogen Energy*. 2024; 75: 557-566. Available from: http://dx.doi.org/10.1016/j.ijhydene.2024.03.313.

[14] Combita-Murcia JD, Romero-Salcedo CA, Montoya OD, Giral-Ramírez DA. Dynamic compensation of active and reactive power in distribution systems through PV-STATCOM and metaheuristic optimization. *Results in Engineering*. 2024; 22: 102195. Available from: http://dx.doi.org/10.1016/j.rineng.2024.102195.

[15] Sakipour R, Abdi H. Voltage stability improvement of wind farms by self-correcting static volt-ampere reactive compensator and energy storage. *International Journal of Electrical Power & Energy Systems*. 2022; 140: 108082. Available from: http://dx.doi.org/10.1016/j.ijepes.2022.108082.

[16] Verma P, Kaimal S, Dwivedi B. Enhancement in fault ride through capabilities with inertia control for DFIG-wind energy conversion system. *International Journal of Ambient Energy*. 2021; 43(1): 6175-6187. Available from: http://dx.doi.org/10.1080/01430750.2021.2000890.

[17] Ranjan M, Shankar R. A literature survey on load frequency control considering renewable energy integration in power system: Recent trends and future prospects. *Journal of Energy Storage*. 2022; 45: 103717. Available from: http://dx.doi.org/10.1016/j.est.2021.103717.

[18] Kadi S, Benbouhenni H, Abdelkarim E, Imarazene K, Berkouk EM. Implementation of third-order sliding mode for power control and maximum power point tracking in DFIG-based wind energy systems. *Energy Reports*. 2023; 10: 3561-3579. Available from: http://dx.doi.org/10.1016/j.egyr.2023.09.187.

[19] Oubrahim Z, Amirat Y, Benbouzid M, Ouassaid M. Power quality disturbances characterization using signal processing and pattern recognition techniques: A comprehensive review. *Energies*. 2023; 16(6): 2685. Available from: http://dx.doi.org/10.3390/en16062685.

[20] Nafeh AA, Heikal A, El-Sehiemy RA, Salem WAA. Intelligent fuzzy-based controllers for voltage stability enhancement of AC-DC micro-grid with D-STATCOM. *Alexandria Engineering Journal*. 2022; 61(3): 2260-2293. Available from: http://dx.doi.org/10.1016/j.aej.2021.07.012.

[21] Akbari S, Taheri M, Taheri A, Ojaghi M. A new reactive power compensation concept for distribution systems using a grid-integrated hybrid photovoltaic/wind turbine system: PV-WT-STATCOM. *International Journal of Circuit Theory and Applications*. 2022; 50(10): 3325-3341. Available from: http://dx.doi.org/10.1002/cta.3338.

[22] Kotla RW, Yarlagadda SR. Mathematical modelling of SPV array by considering the parasitic effects. *SN Applied Sciences*. 2020; 2(1): 50. Available from: http://dx.doi.org/10.1007/s42452-019-1861-x.

[23] Agajie TF, Fopah-Lele A, Amoussou I, Ali A, Khan B, Tanyi E. Optimal design and mathematical modeling of hybrid solar PV-biogas generator with energy storage power generation system in multi-objective function cases. *Sustainability*. 2023; 15(10): 8264. Available from: http://dx.doi.org/10.3390/su15108264.

[24] Anudeep B, Nayak PK, Biswas S. An improved protection scheme for DFIG-based wind farm collector lines. *Electric Power Systems Research*. 2022; 211: 108224. Available from: http://dx.doi.org/10.1016/j.epsr.2022.108224.

[25] Pidikiti T, Shreedevi, Gireesha B, Subbarao M, Krishna VBM. Design and control of Takagi-Sugeno-Kang fuzzy based inverter for power quality improvement in grid-tied PV systems. *Measurement and Sensors*. 2023; 25: 100638. Available from: http://dx.doi.org/10.1016/j.measen.2022.100638.

[26] Anudeep B, Kumar Nayak P. Differential power based selective phase tripping for fault-resilient microgrid. *Journal of Modern Power Systems and Clean Energy*. 2022; 10(2): 459-470. Available from: http://dx.doi.org/10.35833/mpce.2020.000194.

[27] Anudeep B, Nayak PK. Transient energy-based combined fault detector and faulted phase selector for distribution networks with distributed generators. *International Transactions on Electrical Energy Systems*. 2020; 30(4). Available from: http://dx.doi.org/10.1002/2050-7038.12288.

[28] Subbarao M, Dasari K, Duvvuri SS, Prasad KRKV, Narendra BK, Murali Krishna VB. Design, control and performance comparison of PI and ANFIS controllers for BLDC motor driven electric vehicles. *Measurement and Sensors*. 2024; 31: 101001. Available from: http://dx.doi.org/10.1016/j.measen.2023.101001.

[29] Patthi S, Murali Krishna VB, Reddy L, Arandhakar S. Photovoltaic string fault optimization using multi-layer neural network technique. *Results in Engineering*. 2024; 22: 102299. Available from: http://dx.doi.org/10.1016/j.rineng.2024.102299.

[30] Bhatraj A, Salomons E, Housh M. An optimization model for simultaneous design and operation of renewable energy microgrids integrated with water supply systems. *Applied Energy*. 2024; 361: 122879. Available from: http://dx.doi.org/10.1016/j.apenergy.2024.122879.

[31] Yahdou A, Djilali AB, Bounadja E, Benbouhenni H. Using neural network super-twisting sliding mode to improve power control of a dual-rotor wind turbine system in normal and unbalanced grid fault modes. *International Journal of Circuit Theory and Applications*. 2024; 52(9): 4323-4347. Available from: http://dx.doi.org/10.1002/cta.3960.

[32] Li Y, Cao J, Xu Y, Zhu L, Dong ZY. Deep learning based on Transformer architecture for power system short-term voltage stability assessment with class imbalance. *Renewable and Sustainable Energy Reviews*. 2024; 189: 113913. Available from: http://dx.doi.org/10.1016/j.rser.2023.113913.

[33] Govil VK, Sahay K, Tripathi SM. Enhancing power quality through DSTATCOM: a comprehensive review and real-time simulation insights. *Electrical Engineering*. 2024; 106: 7257-7286. Available from: http://dx.doi.org/10.1007/s00202-024-02409-5.